Magneto-electric tuning of the phase of propagating spin waves

Mingqiang Bao,[1] Guodong Zhu,[1,2] Kin L. Wong,[1,a)] Joshua L. Hockel,[3] Mark Lewis,[1] Jing Zhao,[1] Tao Wu,[3] Pedram Khalili Amiri,[1] and Kang L. Wang[1]
[1]*Department of Electrical Engineering, University of California, Los Angeles, California 90095, USA*
[2]*Department of Materials Science, Fudan University, Shanghai 200433, China*
[3]*Department of Mechanical and Aerospace Engineering, University of California, Los Angeles, California 90095, USA*

(Received 19 April 2012; accepted 20 June 2012; published online 11 July 2012)

The utilization of a magnetoelectric film composite to control, by an electric field, the phase of magnetostatic surface spin waves propagating along thin films is reported. Laminates of ferromagnetic films of Ni and NiFe are deposited on a ferroelectric substrate, lead magnesium niobate-lead titanate. The phase of propagating spinwaves is shown to be modulated by an electric field while traveling a finite distance along the surface. The observed phase change in the spinwaves is in agreement with the anisotropy field changes measured with magneto optical Kerr effect hysteresis loops. A quantitative agreement is demonstrated. © *2012 American Institute of Physics*. [http://dx.doi.org/10.1063/1.4734499]

Magneto electric (ME) composite materials consisting of laminate layers of piezoelectric and ferromagnetic materials have received intense attention in recent years (see Refs. 1–3 and references within). In particular, the tuning of the ferromagnetic resonance (FMR) by electric field has been studied in numerous systems.[4–8] The motivation behind such studies is their promising potential for realizing a class of multiferroic microwave devices utilizing electric fields to control the magnetic properties. Here, we report on the electric field modulation of propagating spinwaves with non-zero k-vectors. In contrast to previous FMR experiments with electric field modulation where the spinwaves are generated, modulated, and detected within the same cavity, here spinwaves with finite group velocity are propagating along the surface of a film over distances as large as 8 μm while being modulated by a static electric field causing phase shifts in the spinwaves. This phase shift can be understood as originating from the change in magnetic anisotropy of the ferromagnetic film mediated by mechanical strain coupling to the underlying piezoelectric substrate.

The sample structures used in this study are depicted in Fig. 1. The substrate material is single crystal piezoelectric $[Pb(Mg_{1/3}Nb_{2/3})O_3]_{(1-x)}-[PbTiO_3]_x$ (PMN-PT) ($x \sim 32\%$), cut in the (011) orientation. A ferromagnetic consisting of Ni 40 nm and NiFe 20 nm is sputter deposited onto the substrate and serves as spinwave bus layer. We used permalloy, Ni80Fe20 as material for our spinwave bus. The Ni layer on top of the NiFe serves the purpose of enhancing the magnetoelectric coupling due to the near zero magnetostriction of NiFe.[9–11] The ferromagnetic layers are then covered by 200 nm of SiO_2 deposited by plasma enhanced chemical vapour deposition. Finally, co-planar microstrips of Au are patterned on top of the SiO_2 layer and serve as spinwave generation and detection antennas (Fig. 1). The Au antennas are 4 μm wide and the edge-to-edge separation between the excitation and detection antennas is 8 μm.

The electric field modulation of the magnetic anisotropy is characterized by a magneto-optic Kerr effect (MOKE) setup. The saturation magnetization of our samples is measured by superconducting quantum interference device (SQUID). The spinwaves are generated and detected by a two port network analyzer with each port connected to a closed-loop microstrip antenna, respectively. An external magnetic field applied at an in-plane direction perpendicular to the spinwave propagating direction (surface mode spinwave geometry[12]) is stepped from +1000 Oe to −1000 Oe at a step size of 10 Oe while the network analyzer is sweeping the frequency between 1 to 10 GHz at each magnet step.

The strain response as a function of electric-field of the PMN-PT(011) is well known and shown in Fig. 2 (upper right insert). As the electric field is lowered from the maximum positive value, the strain decreases monotonically until the electric field reaches the critical value ∼−1.5 kV/cm at which point the PMN-PT will begin to be repoled resulting in a huge peak in the strain. Sweeping back the electric field from large negative value to positive ∼+1.5 kV/cm will result again in the repoling of the substrate. When a layer of Ni is deposited onto PMN-PT(011), the strain response can be mapped into a magnetic response due to the magnetostriction of Ni. The Kerr hysteresis loops measured on Ni/PMN-PT(011) as a function of electric field has been studied in detail earlier.[13] Here, we have repeated the same measurements on the structure Ni/NiFe/PMN-PT(011) (Fig. 2). By extracting a scalar parameter, such as the anisotropy field, from such hysteresis loops, the magnetic response can be compared directly with the strain response. The anisotropy field can be extracted from a magnetic hysteresis curve using the peak positions of the second derivative of the magnetization with respect to the applied magnetic field.[14,15] In Fig. 2, we have plotted such derived anisotropy fields as a function of the electric field applied across the PMN-PT(011). A good qualitative correlation of the strain state on the PMN-PT to the extracted anisotropy field can be observed. Especially, prominent peaks near the critical fields of ∼+/−1.5 kV/cm is

a)Author to whom correspondence should be addressed. Electronic mail: kinwong@ee.ucla.edu.

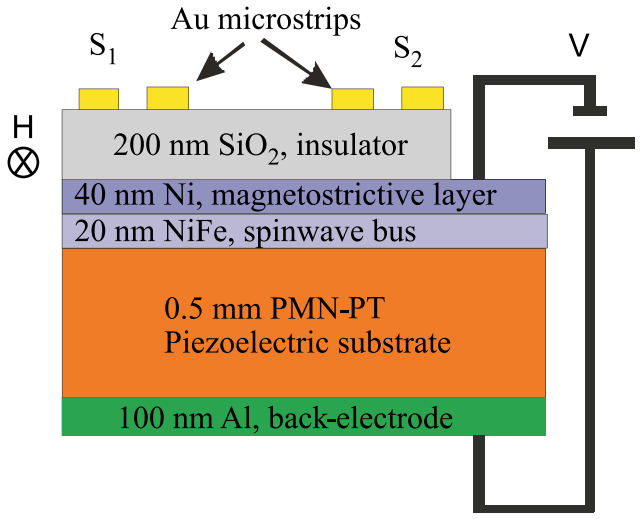

FIG. 1. Cross section of device layer structure and experimental configuration of spinwave excitation (S_1)/detection (S_2) antennas, bias magnetic field, and bias electric field.

observed on both the strain-curve as well as the MOKE anisotropy-curve as the electric field is swept from max to min and vice versa.

The change in the anisotropy field of the MOKE hysteresis curves reflects the strain response of the PMN-PT. A spinwave propagating through such material will, therefore, also experience a change in the magnetic anisotropy as a function of electric field. Unfortunately, Ni is not a good choice for spinwave bus material as it exhibits large Gilbert damping.[16,17] A film of NiFe is, therefore, deposited first onto the PMN-PT substrate to serve as spinwave bus layer based on the known good spinwave properties of NiFe.[11,18] A bilayer structure of Ni/NiFe is needed as NiFe is known to have near zero magnetostriction.

From the Damon and Eschbach equation for surface mode spinwaves,[12,19] the frequencies of the spinwaves are given by (Gaussian units),

$$f^2 = \left(\frac{\gamma}{2\pi}\right)^2 [H^2 + 4\pi M_S H + (2\pi M_S)^2 (2kd)], \qquad (1)$$

where H is the external magnetic field, M_s the saturation magnetization, k the in-plane wavevector of the spinwaves, d the thickness of the ferromagnetic film, and γ the gyromagnetic ratio. Equation (1) assumes the long wavelength limit, i.e., $kd \ll 1$. This is justified for our sample structures as $d = (40 + 20)$ nm while $1/(2\pi k)$ is on the order of eight micrometers as determined by the separation of the antennas.

The S_{21} response measured by the network analyzer is plotted in Fig. 3(a) as a function of both magnetic field and frequency of spinwave excitation. Distinct resonance features are clearly seen. The dispersion of the resonance features fits Eq. (1) well as shown in Fig. 3(b). From the fitting to Eq. (1), we can extract the values of the effective saturation magnetization of the bilayer Ni/NiFe, $M_s = 8$ kG and the bilayer film thickness, $d = 60$ nm. The numbers are confirmed to be in excellent agreement with an independent SQUID measurement performed on the same layered stack structure.

Upon application of an electric field across the PMN-PT, the frequency of the spinwaves changes in accordance with Eq. (1) due to the change in magnetic anisotropy, i.e., $H \rightarrow H_0 + H_k$, where H_0 is the applied magnetic field and H_k is the anisotropy field. This frequency shift is measured as a phase shift by the network analyzer at fixed frequencies. Fig. 4 shows such phase shifts as measured at a fixed frequency of 3.75 GHz. The phase shifts are measured by sweeping the electric field from +4 kV/cm to −4 kV/cm. As the electric field is decreased, the phase increases monotonically. As the electric field decreases further past the critical field (at ∼−1.5 kV/cm), the substrate will begin to be repoled, and we would expect the phase to be low again. This is confirmed by the curve at −4 kV/cm, which is nearly identical with the curve at +4 kV/cm as at these electric fields, the substrate should have the same strain resulting in the same spinwave phase shift.

The phase shift can now be converted into an anisotropy shift according to the following equation:[20]

$$\left.\frac{\partial \varphi}{\partial H}\right|_f \approx -\frac{l}{2\pi M_S d}. \qquad (2)$$

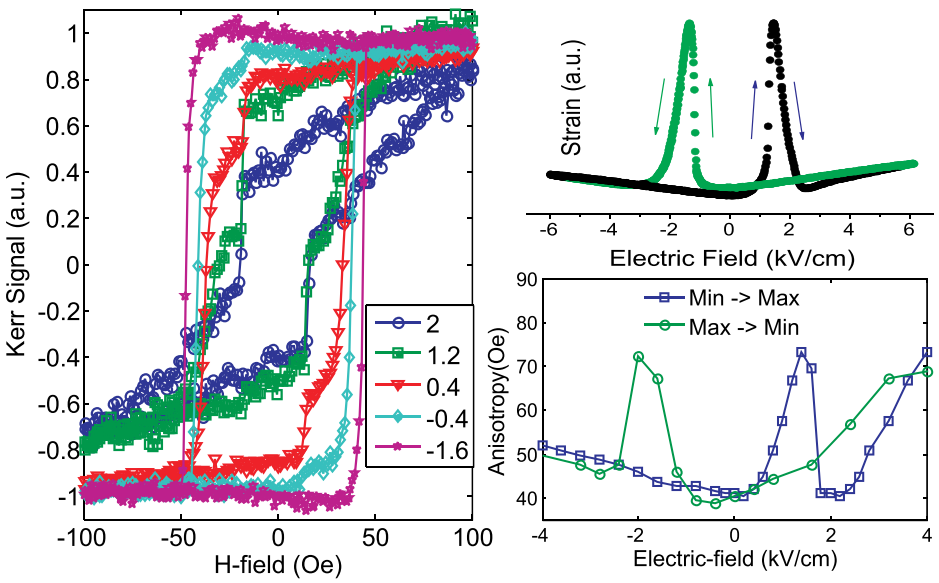

FIG. 2. Left: Kerr hysteresis curves at different electric fields given in units of kV/cm. Upper right: Strain response of PMN-PT as a function of electric field. The arrows indicate the electric field sweeping direction. Lower right: Anisotropy field derived from the MOKE hysteresis curves as a function of electric field.

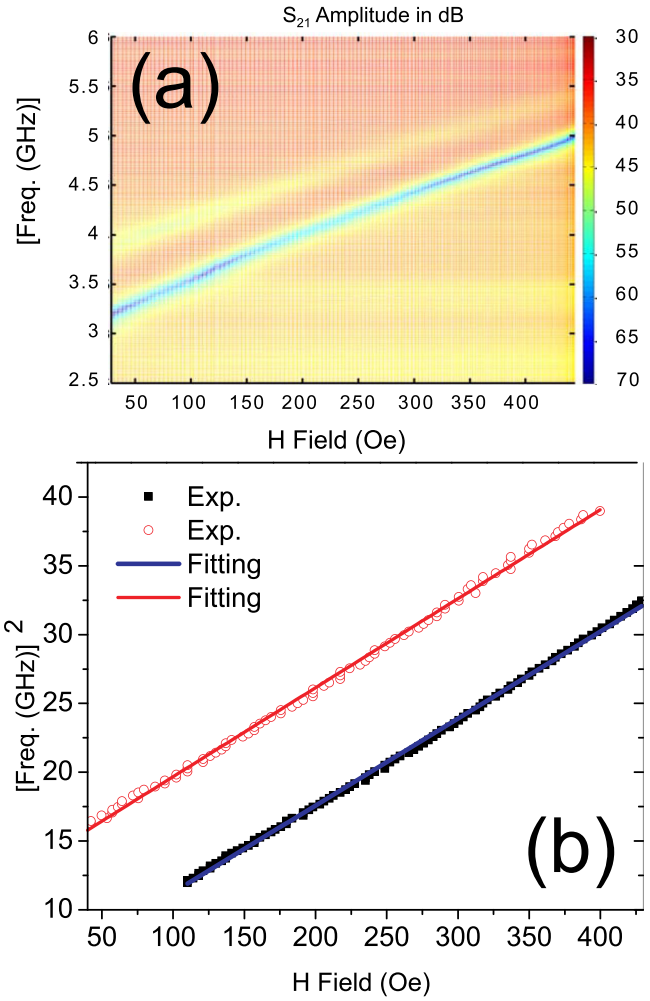

FIG. 3. Top: S_{21} response measured by network analyzer showing the distinct spinwave features. Bottom: Fitting of the experimental data to the Damon and Eschbach surface mode spinwaves.

Here, l is the spinwave travel distance between the excitation and detection antennas. Fig. 5 shows the electric field dependence of such extracted anisotropy shifts for an electric field swept from max, 4 kV/cm to min and

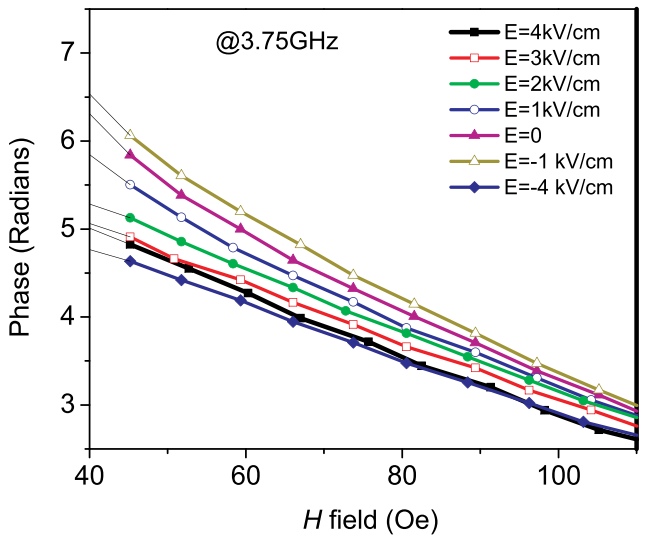

FIG. 4. Measured phase shift of the spinwaves at different electric fields for one fixed frequency.

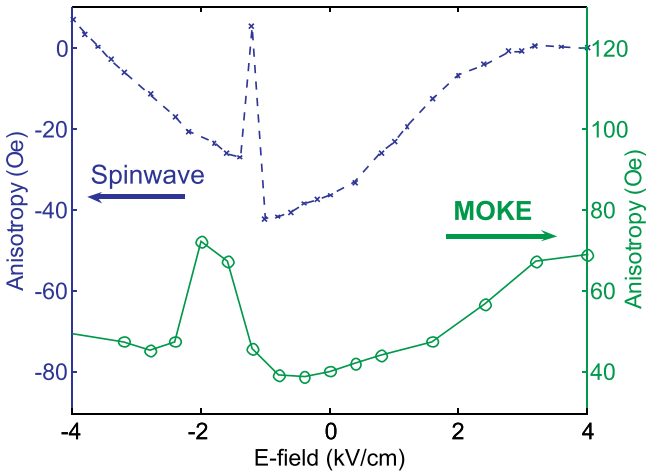

FIG. 5. Left axis: Effective anisotropy field vs electric field derived from spinwave data. Right axis: Effective anisotropy field derived from Kerr hysteresis loops (Fig. 2).

−4 kV/cm value. The figure shows an excellent qualitative resemblance to the strain and magnetic response derived from MOKE data as shown in Fig. 2. The anisotropy field H_k is the sum of intrinsic anisotropy and strain induced anisotropy. The intrinsic anisotropy could be due to shape, crystallinity, and initial poling strain on the PMN-PT substrate. This value is likely to vary from sample to sample especially since the spinwave samples are lithography patterned while the MOKE samples are on the macroscopic scale. The strain induced anisotropy on the other hand depends on the ME-coupling hence on the electric field. The slope of the anisotropy field vs electric field curve should, therefore, represent the magnetoelectric coupling.

From the extracted anisotropy fields, the magnetoelectric coupling coefficient can be derived. Within the linear regime of the strain response (from positive e-field 3 kV/cm to −1 kV/cm), a coefficient of ∼10 Oe cm/kV was obtained. The magnetoelectric coefficients extracted from the Kerr hysteresis loops are on the same order of magnitude at ∼8 Oe cm/kV. The small discrepancy are reasonably within the errors bars of the experiments considering the size of the MOKE samples are considerably larger than the spinwave samples, which may affect the effective strain coupling to the Ni/NiFe layers. The above results supports the interpretation of an one-to-one mapping of the substrate strain to the magnetization state of the Ni/NiFe layer and subsequently the one-to-one mapping of the magnetization state to the effective anisotropy field seen by the propagating spinwaves. The spinwave data also show, within the nonlinear regime near the critical field (∼−1.5 kV/cm) of the PMN-PT, a much higher magnetoelectric coefficient, however the magnetoelectric coupling near the critical field is associated with a large strain peak due to the repoling of the PMN-PT substrate. The repoling process is non-linear, specifically, it exhibits the well known charge vs e-field ferroelectric hysteresis loop. For the linear modulation of spinwave, one should, therefore, stay within the linear regime of the strain respone (e.g., from positive e-field 3 kV/cm to −1 kV/cm).

In summary, we have demonstrated the tuning of the phase of propagating spinwaves by electric field control and the magnitude of the phase change is in excellent agreement with the magnetization change on the Ni/NiFe layers induced by substrate strain. Our experimental findings demonstrate a proof of principle operation of a device for transmission/modulation of information encoded as the phase of spin-waves propagating along a surface.

This work is financially supported by DARPA contract number HR0011-10-C-0153.

[1]J. Ma, J. Hu, Z. Li, and C.-W. Nan, Adv. Mater. **23**, 1062 (2011).
[2]C.-W. Nan, M. I. Bichurin, S. Dong, D. Viehland, and G. Srinivasan, J. Appl. Phys. **103**, 031101 (2008).
[3]G. Srinivasan, in *Annual Review of Materials Research*, edited by D. R. Clarke, M. Ruhle, and F. Zok (Annual Reviews, Palo Alto, 2010), Vol. 40, p. 153.
[4]Y. Chen, A. Yang, M. R. Paudel, S. Stadler, C. Vittoria, and V. G. Harris, Phys. Rev. B **83**, 104406 (2011).
[5]M. Liu, O. Obi, J. Lou, Y. J. Chen, Z. H. Cai, S. Stoute, M. Espanol, M. Lew, X. Situ, K. S. Ziemer *et al*., Adv. Funct. Mater. **19**, 1826 (2009).
[6]J. Lou, M. Liu, D. Reed, Y. H. Ren, and N. X. Sun, Adv. Mater. **21**, 4711 (2009).
[7]Y. Y. Song, J. Das, P. Krivosik, N. Mo, and C. E. Patton, Appl. Phys. Lett. **94**, 182505 (2009).
[8]J. Lou, D. Reed, C. Pettiford, M. Liu, P. Han, S. Dong, and N. X. Sun, Appl. Phys. Lett. **92**, 262502 (2008).
[9]J. P. Reekstin, J. Appl. Phys. **38**, 1449 (1967).
[10]J. Lo, C. Hwang, T. C. Huang, and R. Campbell, IEEE Trans. Magn. **23**, 3065 (1987).
[11]R. Bonin, M. L. Schneider, T. J. Silva, and J. P. Nibarger, J. Appl. Phys. **98**, 123904 (2005).
[12]R. W. Damon and J. R. Eshbach, J. Phys. Chem. Solids **19**, 308 (1961).
[13]T. Wu, A. Bur, K. Wong, J. L. Hockel, C.-J. Hsu, H. K. D. Kim, K. L. Wang, and G. P. Carman, J. Appl. Phys. **109**, 07D732 (2011).
[14]G. Turilli, J. Magn. Magn. Mater. **130**, 377 (1994).
[15]G. Asti and S. Rinaldi, Phys. Rev. Lett. **28**, 1584 (1972).
[16]F. M. F. Rhen, J. F. Godsell, T. O'Donnell, and S. Roy, J. Magn. Magn. Mater. **322**, 1686 (2010).
[17]J. Walowski, M. D. Kaufmann, B. Lenk, C. Hamann, J. McCord, and M. Muenzenberg, J. Phys. D: Appl. Phys. **41**, 164016 (2008).
[18]M. H. Seavey and P. E. Tannenwald, Phys. Rev. Lett. **1**, 168 (1958).
[19]S. O. Demokritov and B. Hillebrands, Spin Dyn. Confined Magn. Struct. I **83**, 65 (2002).
[20]M. Bao, K. Wong, A. Khitun, J. Lee, Z. Hao, K. L. Wang, D. W. Lee, and S. X. Wang, EPL **84**, 27009 (2008).